



Microclimate and its influencing factors in residential public spaces during heat waves: An empirical study in Hong Kong

Yilun Li ^a, Wanlu Ouyang ^b, Shi Yin ^{a,c}, Zheng Tan ^b, Chao Ren ^{a,*}

^a Division of Landscape Architecture, Faculty of Architecture, The University of Hong Kong, Hong Kong SAR, China

^b Department of Building and Real Estate, The Hong Kong Polytechnic University, Hong Kong SAR, China

^c School of Architecture, South China University of Technology, Guangzhou, 510641, China

ARTICLE INFO

Keywords:

Green space
Semi-outdoor space
Subtropical high-density city
Field measurement
Climate-responsive design

ABSTRACT

Creating thermally comfortable living environment under the new normal of heat waves requires pertinent knowledge as references. In subtropical residential areas, various types of public spaces exist, whose microclimate differences during heat waves, as well as their relationship with surrounding building and greenery characteristics, have not been systematically investigated. We therefore evaluated microclimate performances in three typical types of residential public spaces, i.e., open squares, vegetated spaces, and semi-outdoor spaces, and their relationship with surrounding built environment during summertime heat waves. Field measurement of microclimate parameters was conducted in two selected public housing estates in Hong Kong, followed by calculation of thermal comfort indices. Their relationship with building and greenery factors was analyzed. Results show inconsistent patterns in different microclimate variables among three types of spaces across different times of the day, while thermal comfort conditions in the three types of spaces are significantly different. In vegetated spaces and open squares, three-dimensional factors play dominant roles in determining microclimate and thermal comfort condition, with sky view factor (SVF) contributing the most. We detected key SVF threshold for effective thermal comfort enhancement around 0.4, based on which we discussed building and greenery optimization in similar urban context from a point-based SVF perspective and its potential application in practice. In semi-outdoor spaces, two-dimensional land-cover composition contributes greater than three-dimensional factors. This study provides empirical evidence on thermal performance of residential public spaces, which can assist practitioners in achieving adaptation to heat waves in high-density urban contexts in subtropical regions.

1. Introduction

Along with the trend of global warming, heat waves have become the new normal [1]. Though diversely defined worldwide, heat waves generally refer to periods of excessive heat [2]. It is described by World Meteorological Organization as “unusually hot and dry or hot and humid weather that have a subtle onset and cessation”, and “a duration of at least two to three days and a discernible impact on human activities” [3]. Precise criteria on heat waves vary by countries and locations [2], which combines considerations of both physiological and sociological aspects [4]. Nevertheless, the negative impacts of heat waves on the ecosystems and human well-being are globally universal [2]. Challenges are therefore posed to planners and designers when creating thermally comfortable living environment in the face of such extreme heat

conditions, which calls for further knowledge as references [5].

Public spaces in cities are where functional, social and cultural activities occur [6], and residents get exposed to heat stress and risks [7]. Of different types of public spaces, thermal environment in outdoor spaces, e.g., green spaces, urban squares, etc., have been most frequently evaluated [8,9]. To guide planning and design practice, urban morphological indicators were applied to describe two-dimensional (2D) and three-dimensional (3D) building and greenery characteristics [10,11], and their climatic effects were investigated at different scales. At the city scale, empirical studies have been conducted to compare climatic effects of building and greenery [12–15]. Building coverage ratio [12–14] and building height [14] were generally spotted as dominant factors. Buildings’ climatic effect tends to outweigh that of greenery [15], especially when building coverage is high [12]. Such results call for detailed evaluations in different types of land-uses. At the

* Corresponding author.

E-mail address: renchao@hku.hk (C. Ren).

<https://doi.org/10.1016/j.buildenv.2023.110225>

Received 7 January 2023; Received in revised form 3 March 2023; Accepted 18 March 2023

Available online 28 March 2023

0360-1323/© 2023 Elsevier Ltd. All rights reserved.

Nomenclature

Ta	air temperature
Rh	relative humidity
Tmrt	mean radiant temperature
Tg	globe temperature
Tnw	natural wet bulb temperature
v	wind velocity
PET	physiological equivalent temperature
UTCI	universal thermal climate index
HKHI	Hong Kong heat index
SVF	sky view factor
SVF_{building}	sky view factor contributed by buildings
PerT_{20/50}	percentage of tree coverage within 20/50 m buffer zone
PerVG_{20/50}	percentage of ground-level vegetation coverage within 20/50 m buffer zone
PerB_{20/50}	percentage of building coverage within 20/50 m buffer zone
H_{building,20/50}	average building height within 20/50 m buffer zone
H_{tree,20/50}	average tree height within 20/50 m buffer zone

neighborhood scale, factors such as sky view factor (SVF), height-to-width ratio, etc., were found to have significant climatic effects [16]. While when looking into the configuration of building and greenery within a city block at the micro scale, simulation of different design scenarios has been most frequently conducted [17–22]. 3D building morphology indicators were found to perform strong effects on microclimate [17]. Indicators such as building height, floor area ratio, etc., were better correlated with temperature indicators than 2D indicators such as land cover elements ratio [18]. More tree coverage generally provides stronger cooling [19], though such relationship may not be linear [22], and is influenced by configuration of building and trees at micro scale [20,21]. However, rare studies comparing 2D and 3D urban morphology indicators have been based on *in-situ* measurements of microclimate parameters at micro scale [23]. Such evaluation is still needed as it reflects the real situation of thermal environment variation, and provides essential validation to the above-mentioned simulation results.

Besides outdoor spaces, semi-outdoor space, e.g., pilotis, corridors, shelters, shaded terraces, elevated building, sky gardens, etc., is a type of public space widely applied in tropical and subtropical regions, which provides considerable environmental and social benefits [24]. Its thermal environment is related to its intrinsic building forms and spatial attributes [24–26]. Comparisons on thermal environment difference and thermal perception between semi-outdoor space and other types of spaces have been conducted in different urban contexts, e.g., on campus [27–29], around workplace [30,31], in urban parks [32] and public facilities [33], etc. It has been revealed that semi-outdoor spaces are likely to have a restoration effect [30], and provide transient experiences linking indoor and outdoor spaces [34,35]. However, in densely populated residential areas, thermal environment in semi-outdoor spaces, as well as its difference compared to other types of public space, is still in need of investigations. Additionally, besides their intrinsic spatial attributes, how the urban morphology indicators of their immediate surrounding environment influence their thermal environment is still awaiting investigation.

Though some related studies have focused on extreme heat events [36–42], systematic evaluations on thermal environment in different types of public spaces during heat waves are still in rarity. Such evaluation is needed, considering that the characteristics of thermal environment during heat events could be different from those during typical

weather conditions [37,42], as well as their relationship with urban morphology indicators [42]. Such differences may further influence human engagement and behavior [36]. Thus, it is necessary to look into microclimate variance and their relationship with the built environment during heat waves.

During heat waves, microclimate patterns vary across different land uses [41]. Till now, studies have primarily focused on urban green spaces [36–38], with few focusing on densely built residential areas [39]. More pertinent knowledge is needed, as residential areas are closely related to residents' everyday life. As one of the most densely populated cities, Hong Kong features severe and exacerbating heat stress and risks [43,44]. Covering 17 km² of its land [45], Public Housing Estates (PHEs) in Hong Kong accommodate 45.0% of Hong Kong's population [46]. Evaluating thermal environment in PHEs and its influencing factors is important to benefit vast population, and provide useful knowledge to subtropical regions.

In view of these, the objectives of this study are (1) to evaluate the microclimate performance of three typical types of residential public spaces, i.e., open squares, vegetated spaces, and semi-outdoor spaces, during heat waves, and (2) to find out the main influencing factors of the built environment under such urban context. By taking two PHEs in Hong Kong as cases, new evidence given by this study may provide essential knowledge to planners and designers on providing thermally comfortable living environments in subtropical regions, and better adapting to future extreme heat events.

2. Methodology

The workflow of this study is shown in Fig. 1. By taking 2 PHEs in Hong Kong as study sites, field measurement of microclimate parameters was conducted, followed by calculation of thermal comfort indices. Meanwhile, 2D/3D building and greenery factors were measured, and their relationship with microclimate was analyzed. Detailed information is given in the following sections. Additionally, background weather condition during measurement, device calibration method, and detailed information of study site are given in Appendix A-C.

2.1. Study sites

Hong Kong SAR (22°15'N 114°10'E) is located at the south-east coast of China, with a total area of 1106 km². It features a sub-tropical climate with hot and humid summer influenced by monsoon.

Considering locations, construction year, and existence of the targeted public spaces, two typical PHEs, Wo Che Estate and Oi Man Estate, were taken as study sites, as shown in Fig. 2. Located distant from the sea, these two estates feature compact mid-rise buildings, whose heights reach over 50 m, with well-vegetated courtyards as garden spaces. Their basic information is given in Table 1.

2.2. Measurement of microclimate parameters and calculation of thermal comfort indices

2.2.1. Field measurement of microclimate parameters

We conducted field measurement of microclimate parameters on days with “very hot weather warning” announced by Hong Kong Observatory. This extreme high temperature warning is issued based on joint considerations of meteorological data collected from weather stations across Hong Kong, and Hong Kong Heat Index (HKHI), a local empirical index that reflects air temperature, relative humidity, wind condition, and solar radiation [47]. The index is created based on local heat stress and hospitalization data [48], and when it is higher than 30 °C, “very hot weather warning” will be considered. Such local warning system is in line with the physiological and sociological considerations of heat waves, and is therefore taken as the criteria for local heat events.

Air temperature (Ta), relative humidity (Rh), globe temperature

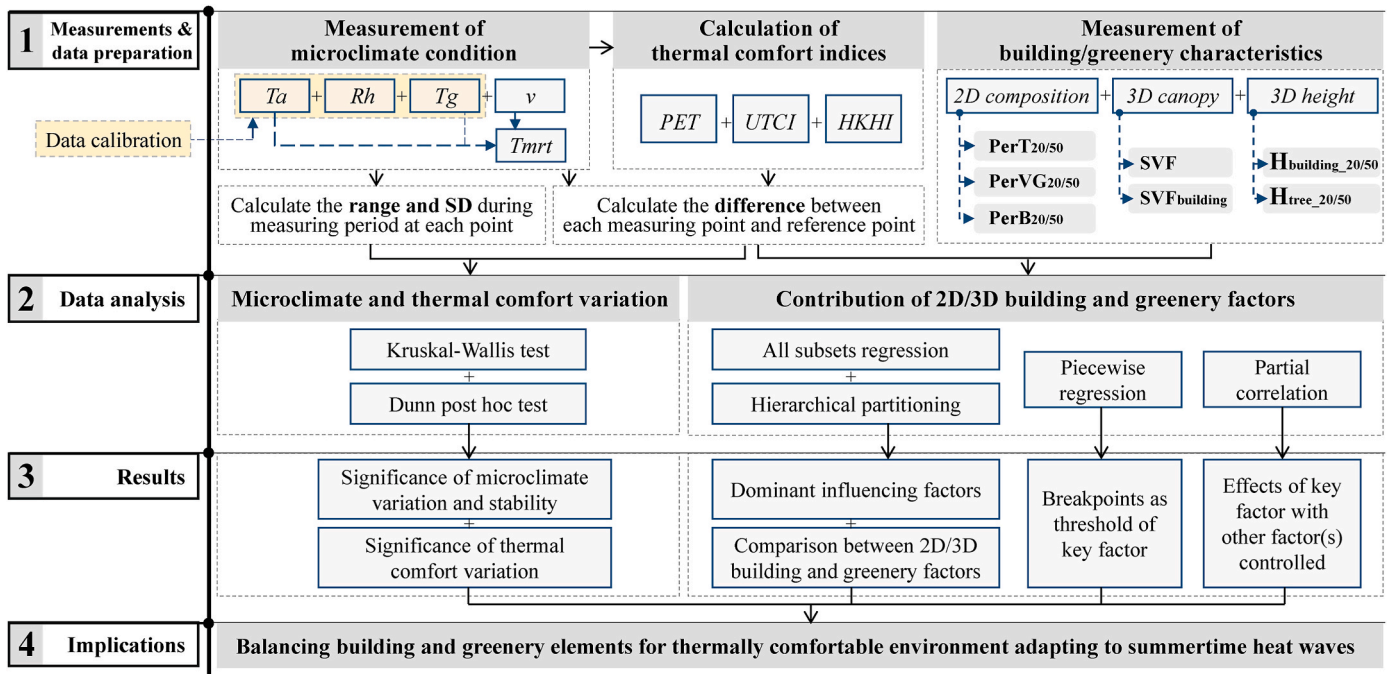


Fig. 1. Workflow of this study.

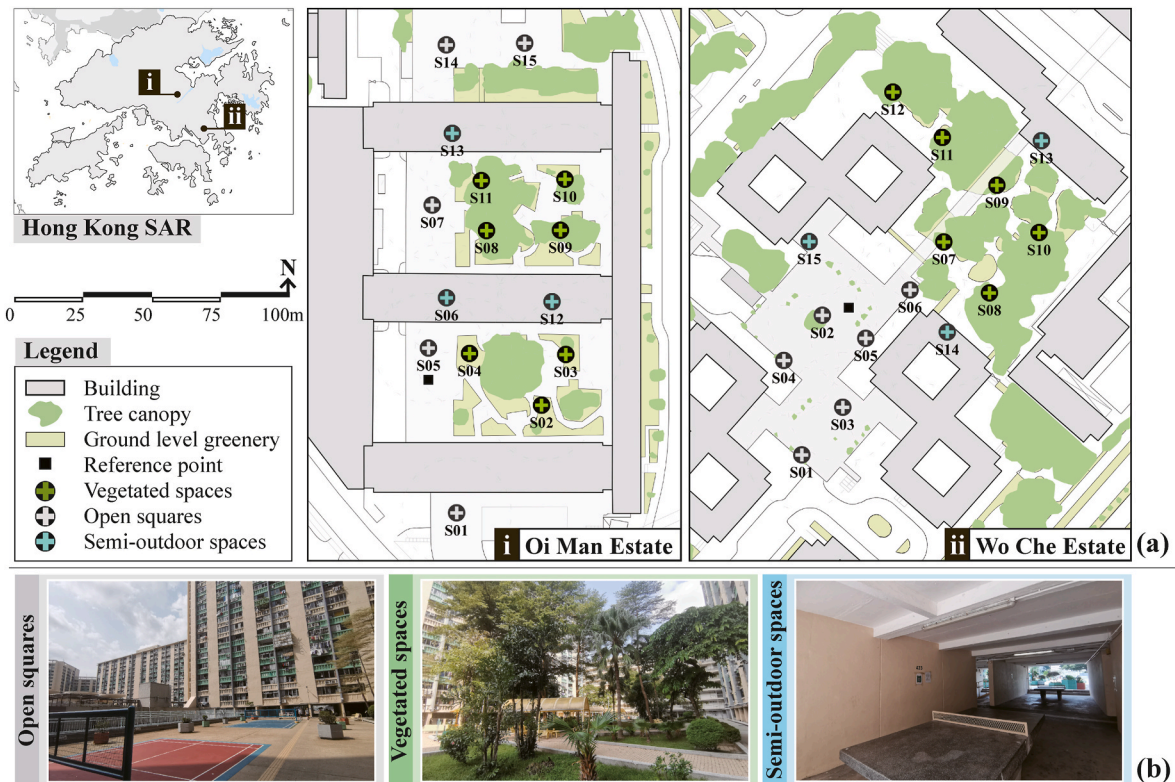


Fig. 2. (a) Locations of study sites and measuring points, and (b) typical examples of three types of public spaces.

(T_g), natural wet bulb temperature (T_{nw}), and wind velocity (v) were measured on summer days during heat waves in 2022, with similar weather conditions of mostly sunny and not windy ($v < 3$ m/s). Measurements during cloudy time were excluded from analysis.

Kestrel 5400 Heat Stress Trackers were used for data collection. The accuracy of the device is ± 0.5 °C for T_a , ± 1.4 °C for T_g , and $\pm 2\%$ for R_h , meeting the requirements of ISO 7726 [49]. Mean radiant

temperature (T_{mrt}) is calculated following equation (1) [50]. This locally recalibrated equation is based on measurements in three typical urban settings, which are open space, tree-shaded spot, and deep street canyon featuring very low SVF, and demonstrated better performance in outdoor environment with the device we utilized.

Table 1

Basic information of selected study sites.

Study site	Built year ^a	Total area ^a	Residents	Green ratio ^b	Building ratio ^b
Wo Che Estate	1977	2584.65	6300	26.85%	22.03%
Oi Man Estate	1974	994.45	6300	20.70%	36.14%

^a Data of the whole Estate. Data source: Housing Bureau, Hong Kong SAR, China.

^b Calculated within each block surrounded by urban roads.

$$T_{mri} = \left[(t_g + 273)^4 + \frac{0.678 \times 10^8 \times v_a^{0.019}}{\varepsilon_g \times D^{0.4}} (t_g - t_a) \right]^{0.25} - 273 \quad (1)$$

where t_g is globe temperature, t_a is air temperature, v_a is wind velocity, D is the globe diameter (0.15 m for Kestrel 5400 Heat Stress Trackers), and ε_g is the emissivity of the black globe (0.95).

One device was located on an open square which is free from the influence of building and tree canopy shades as the reference to record pedestrian-level microclimate conditions within the selected PHEs during 9:30–17:00. Data collected at the reference point is meant to record the microclimate change at the site and eliminate the influence of different measuring time due to the mobile measurement method we adopted. Another three devices were used for mobile measurement across selected measuring points, as shown in Fig. 2(a). These measuring points were selected based on systematic sampling with similar distances among measuring points to the best extent. However, because the three types of spaces are not so spatially evenly distributed within a block, they were adjusted based on the actual situations. Additionally, to exclude unwanted factors such as traffic heat, they were mainly set at the core area of each block away from the adjacent roads. Devices were placed at each measuring point for at least 20min to collect data at 5s intervals, with data collected in the last 10min used for analysis and the rest to ensure device stabilization. Continuous cloudy times were avoided to ensure relatively identical weather condition across different data collection time. To avoid any of the devices used for mobile measurement to be continuously exposed to direct sunshine, the three devices were randomly assigned to measuring points of the three types of spaces. All devices were set at the height of 1.2 m. Three rounds of mobile measurement were carried out during 9:30–17:00, with each representing morning (9:30–11:30), noon (12:30–14:30), and afternoon (15:00–17:00), which covers both typical microclimate measuring time [51] and peak time of residents' outdoor activity [52,53].

Though three identical Kestrel NK5400 were used for mobile measurements in this study, their internal difference would introduce systematic error to results. To reduce such impact, we calibrated measured T_a , R_h , and T_g following [54]. Detailed calibration method is given in Appendix B.

2.2.2. Calculation of thermal comfort indices

Physiological Equivalent Temperature (PET) and Universal Thermal Climate Index (UTCI), two widely used thermal comfort indices [8,55], were calculated. Though demonstrating similar performance [55], the sensitivity of these two indices to green space cooling is slightly different in past local analysis [32,56]. 10-min averaged microclimate parameters were used for the calculation of thermal comfort indices in Rayman Pro [57,58]. Detailed settings are listed in Table D1.

Hong Kong Heat Index (HKHI), an index reflecting local heat stress conditions [48], was calculated following equation (2).

$$HKHI = 0.8 \times T_{mw} + 0.05 \times T_g + 0.15 \times T_a \quad (2)$$

where T_{mw} is natural wet bult temperature, T_g is globe temperature, and T_a is air temperature.

2.3. Measurement of building and greenery factors

As previously introduced, building and greenery characteristics have been quantified through 2D and 3D morphological indicators, and were found having significant impact on urban climate at different scales [10, 11]. Focusing on micro scale within neighborhoods in this study, factors that can directly and comprehensively depict the built environment within a neighborhood are considered, while factors quantifying street canyons such as street orientation, height-width ratio are excluded. Therefore, we deciphered building and greenery characteristics by 2D composition factors and 3D canopy and height factors, as summarized in Table 2 and Fig. 3. These factors describes the composition of different land cover elements, urban canopy structure, and vertical height, and are frequently used in past simulation studies at similar scales and urban settings [18,19].

2D composition was quantified by the coverage ratio of different land cover elements, including tree canopy (PerT), ground-level greening (PerVG), i.e. lawn and shrubs, and building (PerB) within 20 m and 50 m buffer zones (Fig. 3 (a)). Such buffer sizes are effective in analyzing microclimate variations in similar urban context [59].

3D canopy structure was quantified by SVF, which is an urban geometry indicator widely applied in microclimate studies [60]. Fish-eye images taken by Nikon Fisheye Converter FC-E8 mounted on a Nikon COOLPIX800 at the height of 1.2 m were used for SVF calculation in Rayman Pro [57,58]. In order to separate the contribution of building from overall canopy, SVF_{building} was calculated in the same way by using edited fish-eye photographs with tree canopy manually removed, as shown in Fig. 3(b) and C1-2. Though calculation of SVF_{building} based on 3D models is applicable, we adopted this method of manually editing fisheye images for direct comparison with SVF, and for their higher accuracy [60], especially considering the detailed 3D changes around the measuring points. Additionally, such calculation based on edited images corresponds to the sequential design process in practice, which is further discussed in section 4.2.

3D height factors were quantified by mean heights of buildings and trees within 20 m and 50 m buffer zones. The heights of buildings are extracted from governmental data (<https://www.hkmapservice.gov.hk/>), while the heights of trees higher than 4.5 m were field measured by using Nikon Pro II laser rangefinder, and the lower ones were taken as shrubs.

As shown in Fig. 4, collinearity among some factors exists, as all three types of factors provide quantification of building and greenery characteristics. Statistical methods tackling such collinearity are described in Section 2.4.

Table 2

Factors quantifying building and greenery factors.

Influencing Factors		Value range	Unit	Description		
2D	Composition	PerT _{20/50} PerVG _{20/50} PerB _{20/50}	[0,1]	N/A	Percentage of visually interpreted tree canopy, ground-level greening, and building coverage in 20, and 50 m radii buffer zones around each measuring point.	
	3D	Canopy	SVF SVF _{building}	[0,1]	N/A	Overall sky view factor and sky view factor determined by buildings at each measuring point.
		Height	H _{building,20/50} H _{tree,20/50}	[0,+∞)	m	Average building and tree height in 20, and 50 m radii buffer zones around each measuring point.

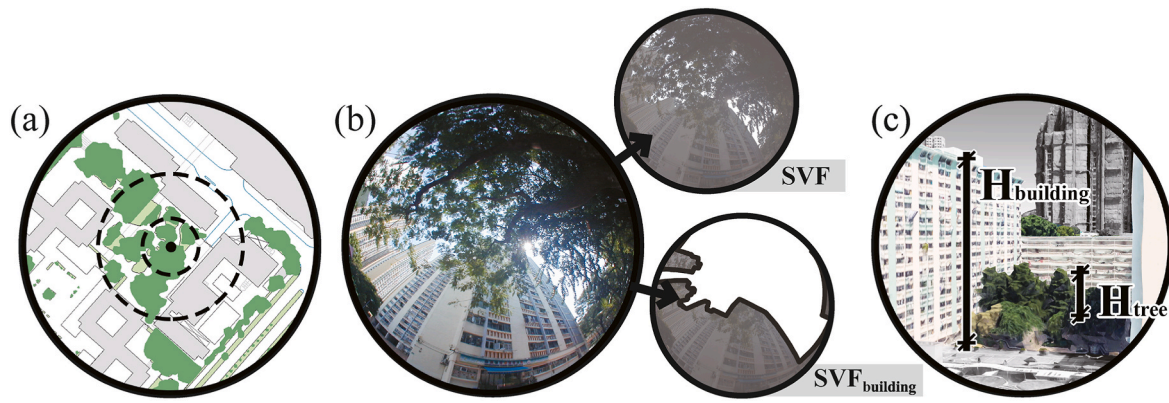


Fig. 3. Calculation of (a) 2D composition factors, (b) 3D canopy factors, and (c) 3D height factors.

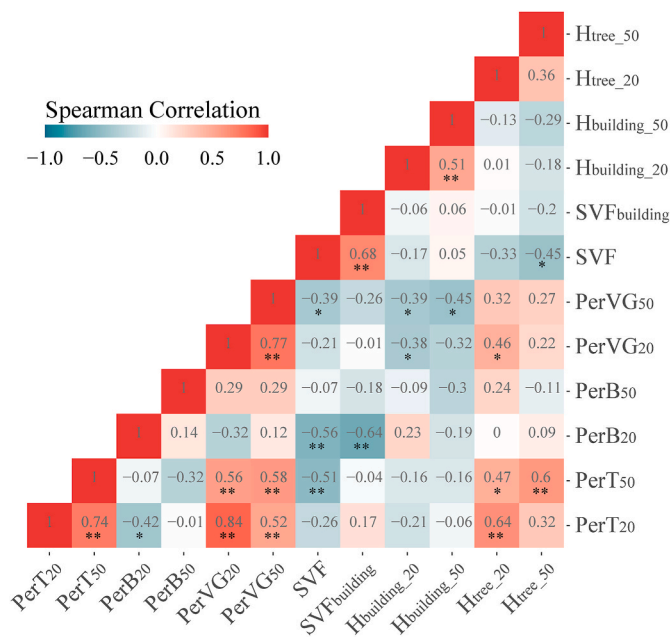


Fig. 4. Spearman correlation coefficient matrix among different factors.

2.4. Data analyses

10-min averaged microclimate parameters at each measuring point were first calculated. To eliminate the influence of different measuring time, Ta, Rh, v, Tmrt, PET, and UTCI differences between the measuring and the reference point were calculated following the below equation,

$$\Delta Parameter = Parameter_{sample} - Parameter_{reference}$$

where $Parameter_{sample}$ is the 10-min average collected at the sampling point, and $Parameter_{reference}$ is the corresponding 10-min average collected at the reference point.

To detect if significant differences exist among different types of spaces, Kruskal-Wallis tests were conducted followed by Dunn post hoc tests. Additionally, to evaluate the stability of microclimate condition, the range, i.e., maximum minus minimum, and standard deviation of each microclimate parameter during 10-min measuring time were calculated. The above-mentioned results are shown in section 3.1.

To evaluate the microclimate effects of 2D/3D building and greenery factors, multiple regression models were built facilitated by performing all subsets regression, and when several significant models were built, Akaike Information Criterion (AIC) was compared to spot the optimal one. To avoid collinearity, one consistent buffer zone size for calculating

2D/3D factors, i.e., 20 m or 50 m, was considered. SVF, instead of SVF_{building}, was used for regression, as the former was calculated from *in-situ* fisheye photos, while the latter was generated from virtual situations.

To further compare the relative contribution of significant factors, we applied hierarchical partitioning, which may identify the independent effects of each factor and alleviate multicollinearity issues [61]. For any factors spotted with primary effects, we applied piecewise regression to detect if key thresholds exist. Piecewise regression introduces breakpoints to linear regression analysis to tackle non-linear but segmented relations [62], which has been used to detect key thresholds in a landscape-level study [63]. Additionally, partial correlation was conducted to evaluate significant correlations with other factors' effects controlled. The above-mentioned results are shown in section 3.2.

All data analyses were conducted in R 4.2.2. R packages FDA, leaps, hier.part, segmented, and ppcor were used.

3. Results

3.1. Microclimate and thermal comfort variation among three types of public spaces

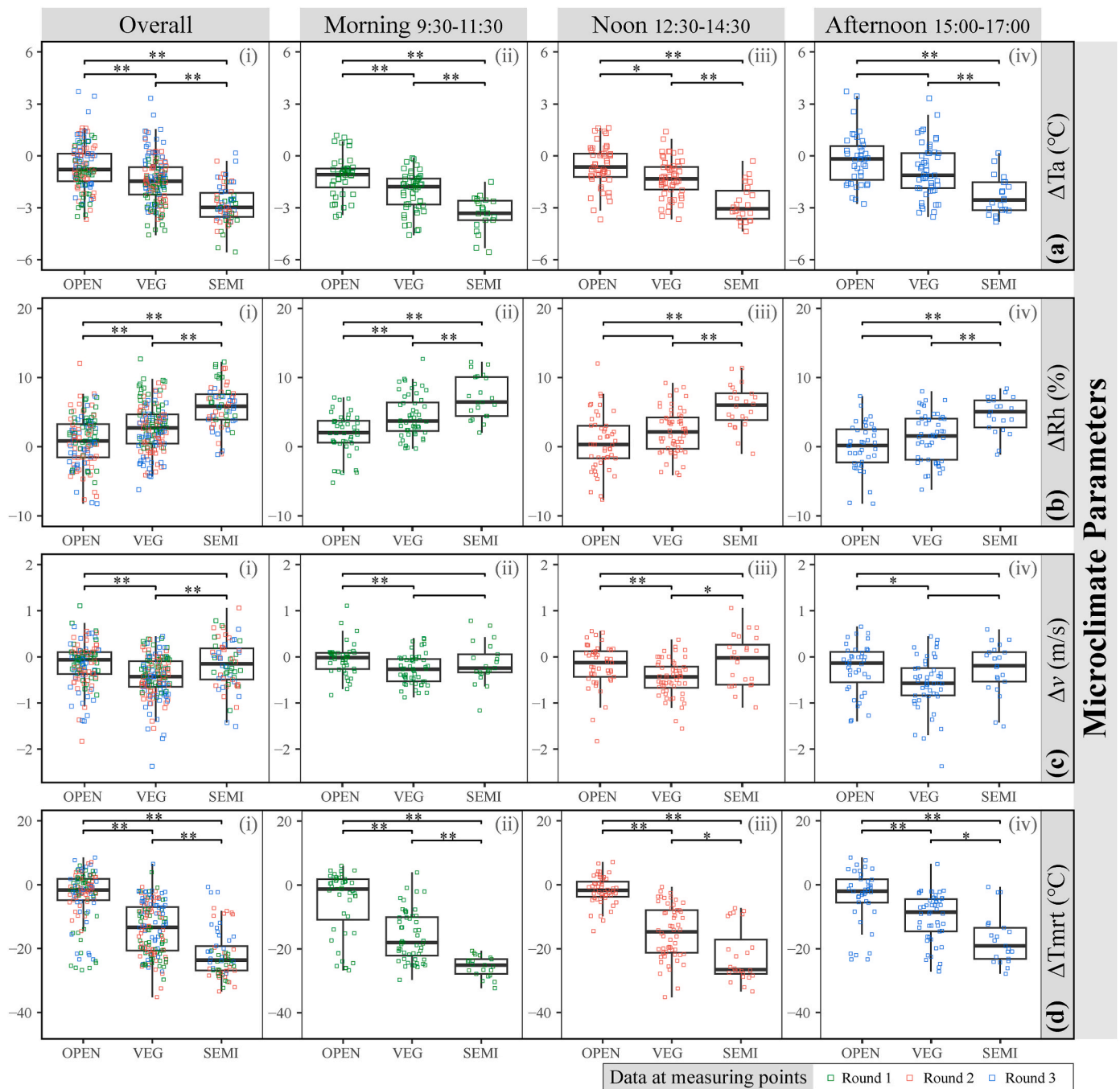
3.1.1. Difference in microclimate condition across different types of spaces

Fig. 5 shows the difference of ΔTa , ΔRh , Δv and $\Delta Tmrt$ among three types of spaces. Detailed descriptive statistics are given in Table E1. By comparing to samples on open squares, the difference in mean overall ΔTa , ΔRh , Δv , and $\Delta Tmrt$ in vegetated and semi-outdoor spaces are 0.75 °C, 1.85%, 0.27 m/s, 13.63 °C, and 2.14 °C, 5.01%, 0 m/s, 22.34 °C respectively (Table E1). Significant differences in ΔTa , ΔRh and $\Delta Tmrt$ among three types of spaces exist while varying across measuring time (Fig. 5). For example, differences in ΔTa and ΔRh between open squares and vegetated spaces are insignificant in the afternoon. In terms of Δv , a significant difference exists between open squares and vegetated spaces across all periods, while that of open squares and semi-outdoor spaces are always insignificant.

Fig. 6 shows the range (Fig. 6 (i)-(iv)) and standard deviation (Fig. 6 (v)-(viii)) of measured microclimate parameters during the 10-min measurements at each point. Significant differences among three types of spaces are consistently detected, indicating differences in microclimate stability among three types of spaces. Ta, Rh and Tmrt are most stable in semi-outdoor spaces, compared to vegetated spaces and open squares. In terms of v, vegetated spaces are significantly more stable than open squares and semi-outdoor spaces, differences among which are statistically insignificant (Fig. 6 (iii), (vii)).

3.1.2. Difference in thermal comfort across different types of spaces

Fig. 7 demonstrates consistently significant differences in thermal comfort and heat stress indices among three types of spaces. Detailed



Microclimate Parameters

Fig. 5. ΔT_a , ΔR_h , Δv and ΔT_{mrt} variance among 3 types of public spaces at different time of the day. (Note: * and ** refer to significant differences between groups at $\alpha = 0.05$ (two-tailed) and $\alpha = 0.01$ (two-tailed) respectively.).

descriptive statistics are given in Table E2. Across all three measuring times, the difference in thermal comfort indices is always the highest in semi-outdoor spaces and the lowest in open squares, indicating least thermal comfort condition in open squares. The mean overall enhancement of thermal comfort in vegetated and semi-outdoor spaces compared to open squares are 4.95 °C and 10.28 °C in PET, 2.95 °C and 6.65 °C in UTCI, and 1.48 °C and 2.84 °C in HKHI (Table E2). The three evaluated thermal comfort indicators show similar temporal patterns, the mean thermal comfort difference was always the largest in the morning, while the smallest in the late afternoon except for ΔPET in open squares.

To directly demonstrate the thermal comfort conditions in three types of spaces during heat waves, Fig. 8 demonstrates the absolute

value of thermal comfort indices at each measuring point, as well as those calculated at the reference point of the same measuring time. Though different indices were applied, compared to the corresponding heat acceptability thresholds, similar trends were shown. In open squares, 78.79% (PET), 80.80% (UTCI), and 72.72% (HKHI) of calculated thermal comfort indices at measuring points were beyond the corresponding heat acceptability threshold. In vegetated spaces, such proportions are much less, which are 29.30% (PET), 36.89% (UTCI), and 21.66% (HKHI). Thermal comfort in semi-outdoor spaces were consistently most preferable, with all calculated indices lower than the local heat acceptability thresholds.

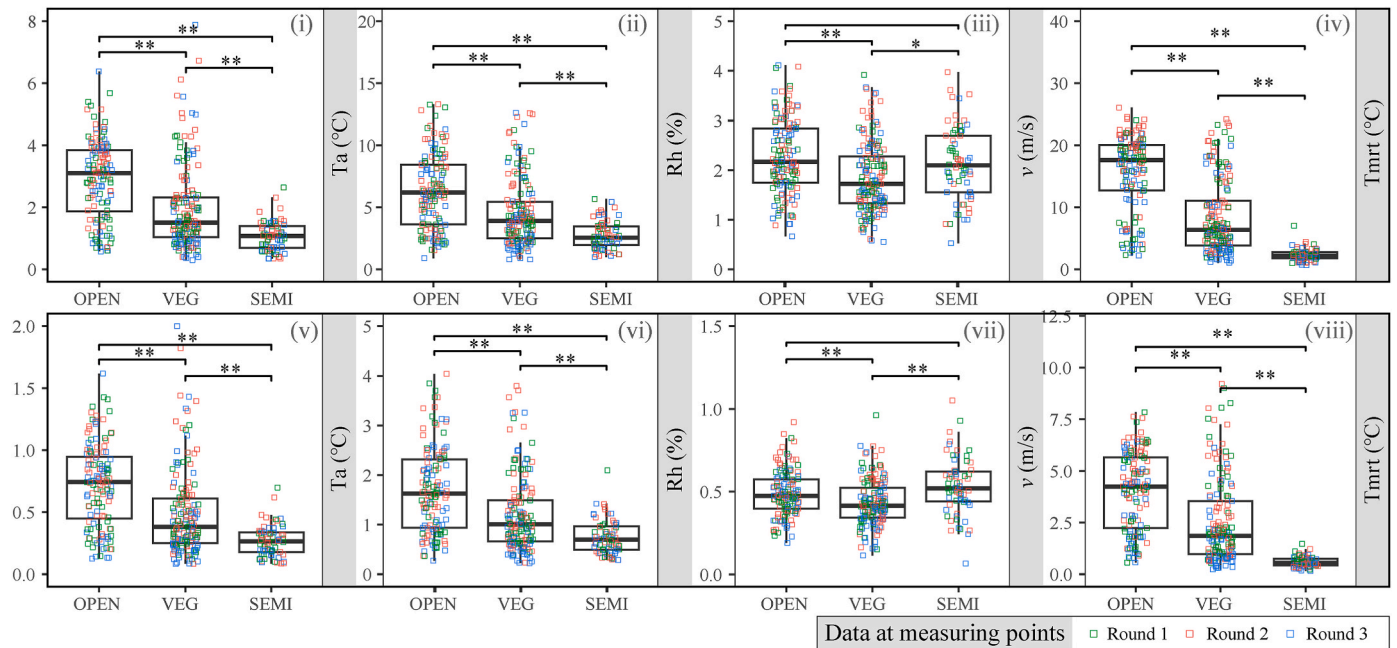


Fig. 6. Range and standard deviation of measured T_a , R_h , v , and T_{mrt} during 10 min measuring at each measuring point. (Note: * and ** refer to significant differences between groups at $\alpha = 0.05$ (two-tailed) and $\alpha = 0.01$ (two-tailed) respectively.).

3.2. Contribution of 2D/3D building and greenery factors

3.2.1. Dominant factors in different types of spaces

Using all subsets regression, optimal regression models were built with 2D/3D building and greenery factors as independent variables. Fig. 9 demonstrates the effects of these factors on microclimate and thermal comfort parameters in different types of spaces. Among all factors, SVF is most included. As SVF increases, i.e., more views of sky, ΔT_a , ΔT_{mrt} , ΔPET , $\Delta UTCI$, and $\Delta HKHI$ increase, while ΔR_h decreases. Increasing coverage of ground-level vegetation ($PerVG_{50}$) and building coverage ($PerB_{50}$) may enhance thermal comfort in semi-outdoor spaces, while the opposite trend applies for tree canopy coverage ($PerT_{50}$). Microclimate effects of building height ($H_{building_{50}}$) vary across different types of spaces, increasing which may enhance thermal comfort on open squares, while may deteriorate that in semi-outdoor spaces. No significant multiple regression models were built for thermal comfort indices in vegetated spaces. Details of these models are presented in Appendix F.

Based on the optimal regression models, Fig. 10 shows the independent effects of each factor quantified by hierarchical partitioning. It is shown that in outdoor spaces, i.e., open squares and vegetated spaces, 3D canopy and height factors generally play dominant roles in determining microclimate and thermal comfort conditions (Fig. 10 (a-f)/ii, iii), with SVF and $H_{tree_{20/50}}$ most included. While in semi-outdoor spaces, 2D composition factors perform greater independent effects (Fig. 10 (a-f)/iv). When considering all three types of spaces, SVF consistently contributes the most independent effect (Fig. 10 (a-f)/i).

Fig. 10 also shows the accumulative independent effects of building and greenery factors. In semi-outdoor spaces, building factors generally performs greater effects than greenery, while the opposite trend applies to open squares. However, due to the significant effect of SVF, building and greenery's accumulative contribution are low in vegetated spaces and when all types of spaces are taken as a whole.

3.2.2. Effects of SVF on thermal environment in outdoor spaces

As SVF serves as the dominant influencing factor in outdoor spaces, i.e., open squares and vegetated spaces, we further look into how microclimate and thermal comfort indices in outdoor spaces respond to SVF jointly. As shown in Fig. 11, ΔT_a , ΔT_{mrt} , ΔPET , $\Delta UTCI$, and $\Delta HKHI$

gradually increase as SVF increases, while the relation seems not simply linear. The opposite trend applies for ΔR_h . By using piecewise regression, significant breakpoints were found for all parameters (Fig. 11). For ΔT_a and ΔR_h , breakpoints exist at $SVF = 0.291$ (Fig. 11(a), (b)), while for ΔT_{mrt} , ΔPET , $\Delta UTCI$, and $\Delta HKHI$, breakpoints exist around $SVF = 0.4$ (Fig. 11(c)–(f)).

We further break down the effect of SVF contributed by building and greenery through partial correlation. As shown in Table 3, when outdoor spaces are taken as a whole, significant correlations persist even if the effects of $SVF_{building}$ are controlled, indicating weak microclimate effects of SVF contributed by buildings. When looking into one specific type of space, similar results are obtained in vegetated spaces, while opposite on open squares. For ΔT_{mrt} , ΔPET , $\Delta UTCI$, and $\Delta HKHI$ in open squares, insignificant correlations with SVF were detected when controlling the effects of $SVF_{building}$, indicating weak effects of greenery elements on thermal comfort condition.

4. Discussion

4.1. Thermal environment diversity in densely built-up residential areas during heat waves

Three types of residential public spaces show highly diversified microclimate and thermal comfort conditions during summertime heat waves (Figs. 5–7). Though the selected measuring points are spatially close (Fig. 2), considering that the thermal properties of different underlying surfaces vary greatly [67], microclimate and thermal comfort variation could be large even in very close vicinity [68]. Such variation in the thermal environment is likely to be intensified during heat waves, as the mean overall ΔT_a , ΔPET , and $\Delta UTCI$ difference between vegetated and open squares (T_a 0.75 °C, PET 6.75 °C, $UTCI$ 3.75 °C) are stronger than a similar local study [32]. Such intensification is in line with the microclimate variance under different subtropical synoptic condition [42].

Among the three types of public spaces, semi-outdoor spaces demonstrate the highest potential to provide a thermally comfortable environment during heat waves, with all calculated thermal comfort indices falling within the range of local heat acceptability (Fig. 8).

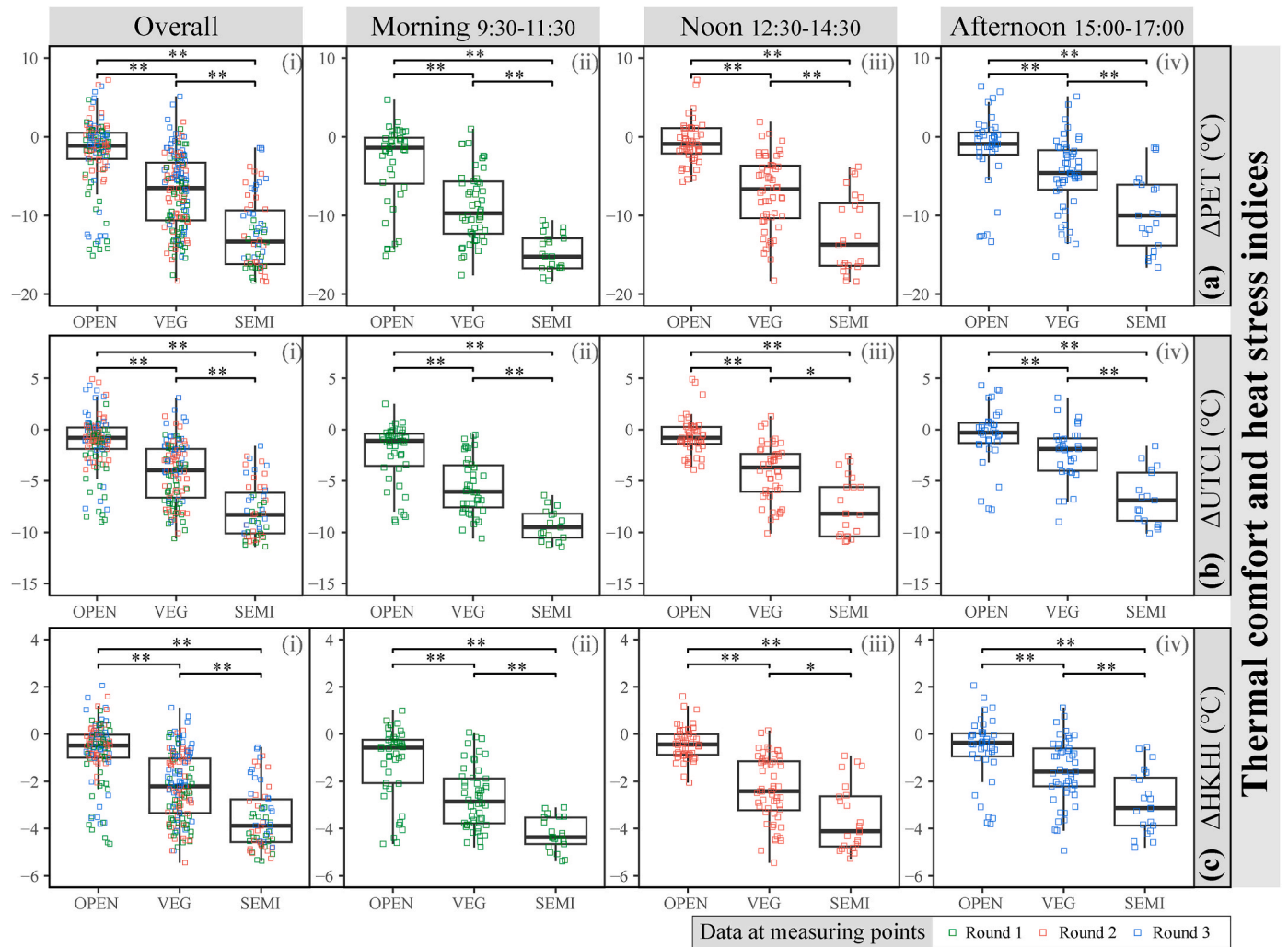


Fig. 7. Δ PET, Δ UTCI and Δ HKHI variances among 3 types of public spaces at different time of the day. (Note: * and ** refer to significant differences between groups at $\alpha = 0.05$ (two-tailed) and $\alpha = 0.01$ (two-tailed) respectively.).

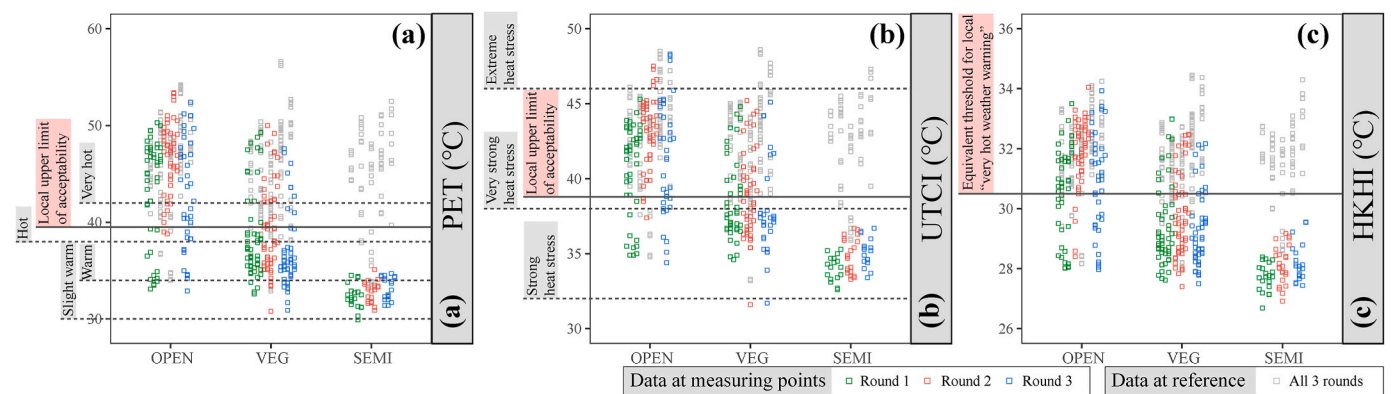


Fig. 8. (a)PET, (b)UTCI and (c)HKHI in three types of spaces at different time of the day. (Note: Local upper limit of heat acceptability quantified by PET (39.5 °C) and UTCI (38.8 °C) derives from Ref. [64], and equivalent threshold for local “very hot weather warning” derives from Ref. [48]. Thermal stress classification on PET and UTCI scale are based on [65,66].).

Significant shading provided by buildings guarantees the alleviation of heat stress [69], especially considering that these spaces are not exposed to sun exposure, i.e., with no direct solar energy intake. This may explain why the enhancement of thermal comfort in semi-outdoor spaces is stronger than that in vegetated spaces in this study.

However, the wind amplification effect in semi-outdoor spaces [69] compared to open squares was not observed (Fig. 5 (c)), and an opposite trend of thermal comfort enhancement between semi-outdoor and vegetated spaces compared to Ref. [32] was observed, which may largely due to their different urban settings and different spatial

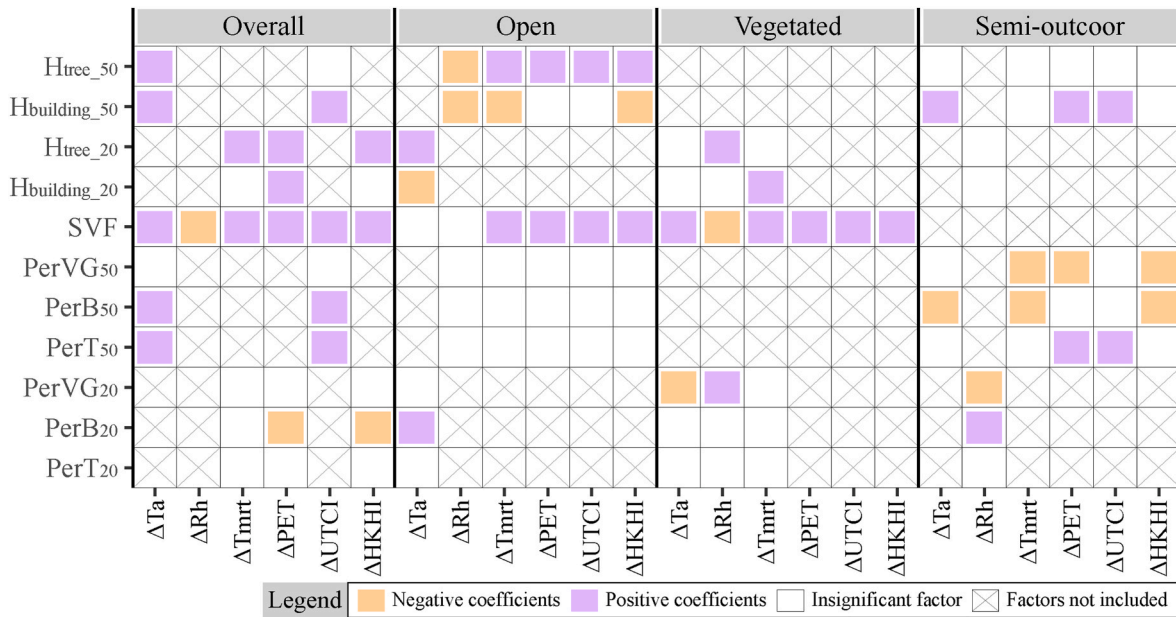


Fig. 9. Summary on coefficients of optimal linear regression models with 2D/3D building and greenery factors as independent variables and microclimate and thermal comfort indices as dependent variables. (Note: In each column, crossed parameters are not included in building linear models, as one consistent buffer zone is considered in building one model. SVF is excluded from models for semi-outdoor spaces, as it equals 0 at all semi-outdoor measuring points.)

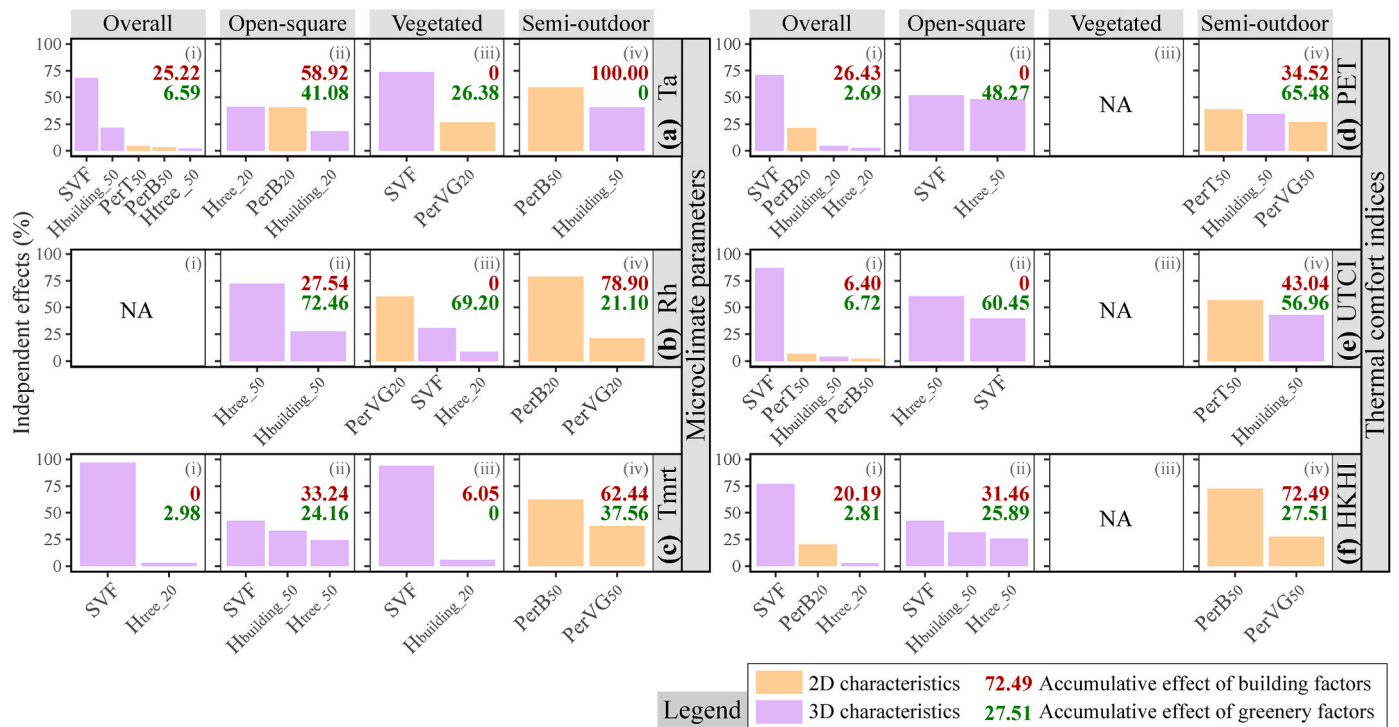


Fig. 10. Independent effect of 2D/3D building and greenery factors by using hierarchical partitioning. (Note: NA indicates no significant multiple regression models built for the microclimate/thermal comfort parameter in the particular type of space(s).)

attributes of these semi-outdoor spaces. Additionally, this empirical study under the context of heat waves may supplement the results of past studies under typical summer condition [69,70], and support the advocacy of utilizing semi-outdoor spaces in tropical and subtropical high-density cities to provide thermally comfortable environment [69, 71].

4.2. Dominant 2D/3D building and greenery factors to guide design practice

During heat waves, microclimate conditions vary across different land-uses due to their different urban spatial forms [41]. Focusing solely on residential areas, the multiple regression models built in this study (Fig. 9) reconfirms that microclimate and thermal comfort are sensitive to building and greenery elements in close vicinity [72].

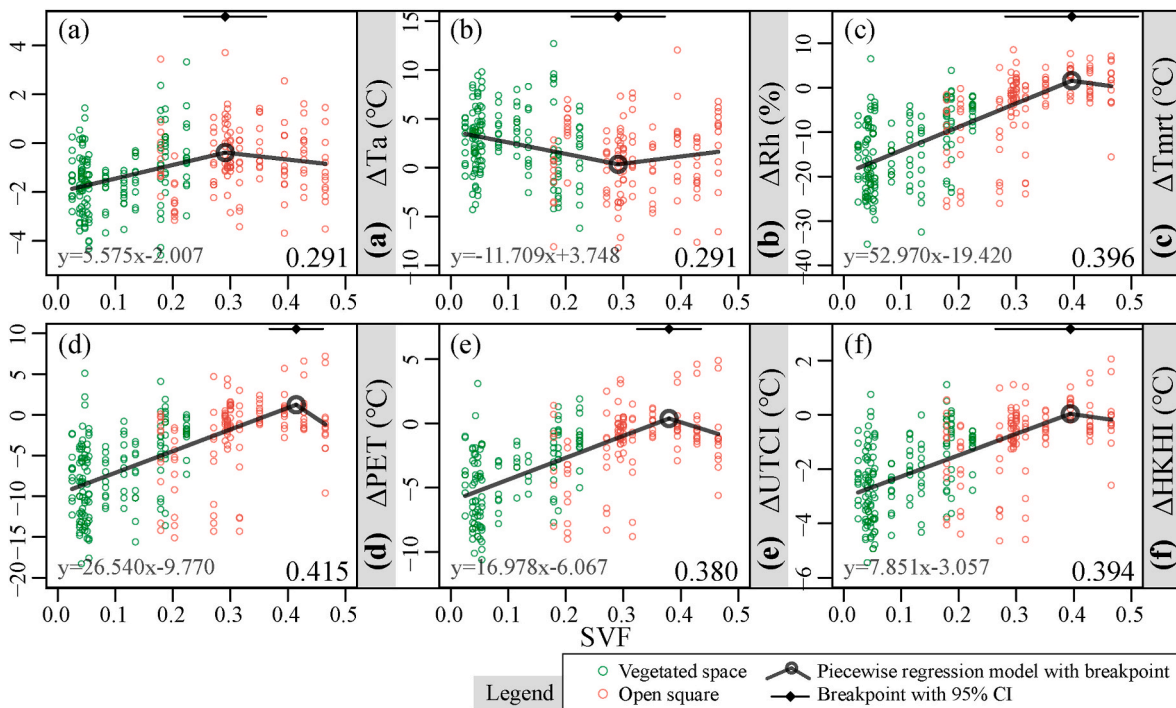


Fig. 11. Detected break points by piecewise regression between microclimate parameters, thermal comfort indices and SVF in outdoor spaces. (Note: Numbers at the right bottom are detected breakpoints.)

Table 3

Spearman’s correlation and partial Spearman’s correlation with SVF_{building} controlled between microclimate parameters, thermal comfort indices and SVF in outdoor spaces.

		Microclimate parameters			Thermal comfort indices		
		ΔT_a	ΔRh	ΔT_{mrt}	ΔPET	$\Delta UTCI$	$\Delta HKHI$
Vegetated and open square	ρ	0.338**	-0.235**	0.656**	0.714**	0.718**	0.611**
	Par ρ	0.337**	-0.248**	0.656**	0.671**	0.654**	0.582**
	n	289			247		289
Vegetated	ρ	0.251**	-0.138	0.433**	0.453**	0.532**	0.421**
	Par ρ	0.192*	-0.064	0.373**	0.408**	0.494**	0.372**
	n	157			122		157
Open-square	ρ	0.049	0.081	0.522**	0.576**	0.466**	0.307**
	Par ρ	-0.185*	0.259**	0.072	0.068	-0.006	-0.089
	n	132			125		132

Note: ρ Spearman’s correlation, **Par ρ** Partial Spearman’s correlation with SVF_{building} controlled, **n** sample size. * and ** refer to significant correlation at $\alpha = 0.05$ (two-tailed) and $\alpha = 0.01$ (two-tailed) respectively.

In semi-outdoor spaces, dominant influencing factors are 2D compositional ones (Fig. 10). While in outdoor spaces, 3D canopy and height factors play dominant roles, with building factors contributing more to thermal environment variation (Fig. 10). Such results are in line with past studies based on numerical simulation [17,18], though different 3D indicators describing vertical building morphology were utilized. Comparatively, the coverage of vegetation elements was only included in models of ΔT_a and ΔRh in vegetated spaces, indicating a less significant contribution of 2D vegetation composition. Such results differ from previous understanding of the strong cooling effects of vegetation [19–21], especially tree canopy during heat waves [39]. Besides weaker climatic effects compared to buildings, what may also explain this, is that SVF partly includes description of tree canopy information, as shown in Fig. 4 the strong correlation between SVF and PerT₅₀ ($\rho = -0.51$). However, considering that they describe different aspects of urban morphology, 3D canopy and 2D composition factors were included in multiple regression models. Tree canopy’s contribution to SVF is demonstrated in Table 3, which we find may guide design practice in residential contexts, as discussed in section 4.2.1. Such

comparisons on 2D/3D characteristics may supplement those studies under the city scale [12–14] and provide reference to allocating building and greenery elements in residential areas at the micro scale.

Based on the above-mentioned dominant influencing factors in different types of spaces, implications for balancing building and greenery elements in outdoor and semi-outdoor spaces are given below.

4.2.1. SVF as a key indicator for building and greenery configuration in outdoor spaces

In residential areas, outdoor spaces are composed of building and greenery elements, whose interactions have an impact on microclimate condition [12,73]. In this microscale study conducted within urban blocks of subtropical high-density urban setting, 3D canopy factor SVF plays a dominant role on outdoor thermal environment (Fig. 10), which strengthens the significance of shading [74], especially under high-temperature heat waves.

The non-linear relationship between SVF and thermal comfort indices yields a threshold of around 0.4, below which thermal comfort can be effectively enhanced. This threshold shows up on open squares

(Fig. 11), indicating that thermally comfortable environment under high-temperature heat waves may exist in spaces whose SVF are mainly contributed by buildings. Allocating tree canopies or other shading infrastructures to such spaces would be less efficient than allocating them to spaces with SVF over the threshold, which may avoid the SVF contributed by landscape elements be lost to that contributed by buildings. Similarly, in studies conducted in comparable contexts, trees' shading may largely be lost to the shades of buildings in densely built-up area [20,75], though greenery's shading was found more significant than building's shade [76].

As SVF is determined by building and greenery elements jointly, to decompose their contribution, we adopted two factors, i.e., SVF and SVF_{building} . Different from past studies of extracting different elements from the same image [77–79], we calculated SVF contributed solely by buildings through manually edited fisheye images. This method echoes the procedure in design practice, with architecture design framing the spaces first, followed by landscape design in outdoor areas. Corresponding to this procedure, SVF is first determined by spatial arrangements of buildings, and then contributed by tree canopy and other shading infrastructure in landscape.

Based on these, an SVF threshold perspective shows the potentials to guide the configuration of greenery within urban blocks of similar high-density urban context. For areas whose SVF_{building} are lower than the SVF threshold, open squares and related functions can be prioritized. While for vegetated spaces, tree optimization shows potentials to achieve best SVF reduction, as shown in Fig. 12 a point-based illustration of how different tree configuration of same sets of trees (Fig. 12 (b), (c)) may lead to different 3D canopy condition under certain building settings. Considering that changing tree locations surrounding one point may also influence SVF of its' adjacencies, optimization of greenery could be obtained by applying such point-based analysis to an area of interest through splitting into grids and calculating SVF in each grid. For example, this could help to optimize the tree canopy configuration in urban renewal projects with similar site condition, when new trees could be planted, or current trees could be moved to new places. Meanwhile, we find this may help go beyond restrictions on coverage ratio [22] and simple planting patterns, e.g., trees in lines and squares, etc., in past parametric studies [80], and provide reference to more complex configurations of different vegetation types as in practice. We propose such an SVF perspective for building and greenery optimization awaiting

future validation.

4.2.2. Land cover composition as an important indicator in semi-outdoor spaces

In semi-outdoor spaces, their intrinsic spatial attributes, summarized as porosity, openness, and exposure, were decisive in their thermal performance [24–26]. Supplement to that, we found that the land cover in the adjacent buffer zones may also have a significant influence (Fig. 9). We found that increasing building and ground-level greenery coverage may enhance the thermal comfort in semi-outdoor spaces. As all semi-outdoor spaces are located at ground floors of buildings, improving buildings coverage can be seen the same as enhancing the size of these semi-outdoor spaces, which creates more constantly building-shaded areas. And by enhancing the ground-level greenery coverage, pavement will be replaced by pervious surfaces, and air will be less heated before ventilated to semi-outdoor spaces. However, contrary to intuition, enhancing tree canopy coverage was found to have a negative effect on thermal comfort. It may be explained that almost all selected semi-outdoor spaces in this study are directly connected to open squares, as they are mostly exits of these buildings. It makes these semi-outdoor spaces less influenced by the cooling of tree canopies. Additionally, ventilation is important in improving the thermal comfort in semi-outdoor spaces [69]. Though enhancing tree canopy coverage is effective in regulating microclimate through providing shades [81], we find that dense vegetation may decrease the air flow, as vegetated spaces feature significantly lower wind speed (Fig. 5 (c)). Additionally, heated airflow under extreme heat condition could also possibly perform a negative effect on human [82], and seems humidity-dependent [83]. How wind condition influences thermal comfort condition in public spaces under extreme heat still awaits future validation.

Though results in this study indicate the significance of land cover composition around semi-outdoor spaces, we are unable to compare its significance to the intrinsic spatial attributes of these semi-outdoor spaces, as all sampled spaces are ground-floor pilotis with similar depth and height belonging to the horizontal breezeway defined by Gamero-Salinas et al. [24]. To find answer to this question, future assessment by including different kinds of semi-outdoor spaces is needed.

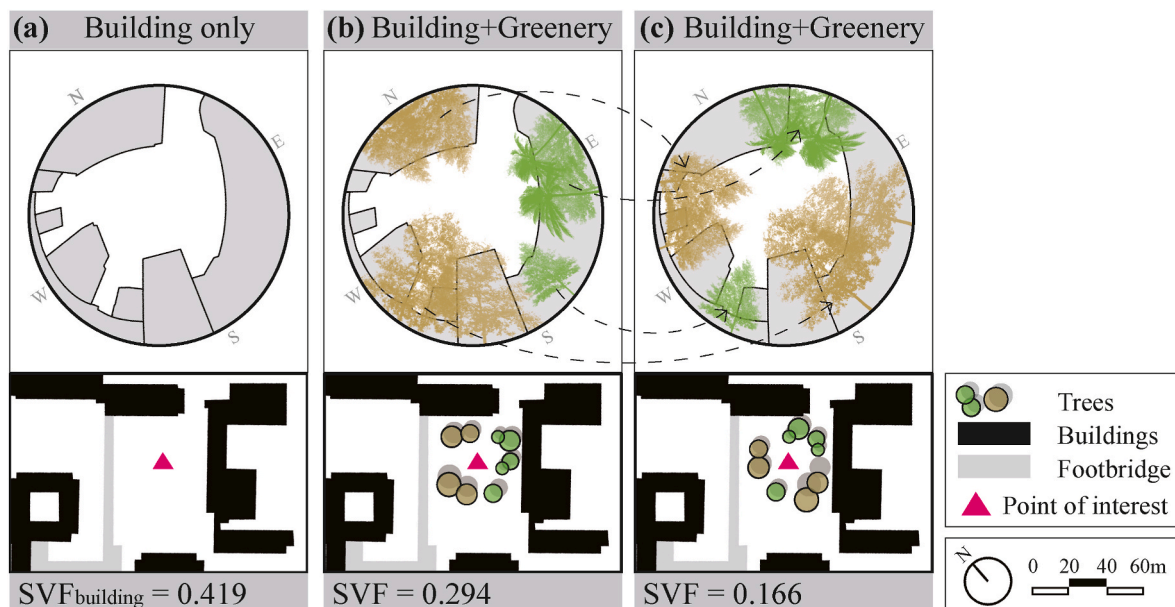


Fig. 12. Illustration of a point based SVF perspective for building and greenery optimization. Note: Values of SVF are calculated by using Rayman Pro. This illustration is based on S10 in Wo Che Estate.

4.3. Limitations

We consider the below limitations that could be enhanced in future work. Firstly, by adopting a mobile measurement method, field measurement in this study is limited by temporal and spatial resolution, as well as the accuracy of the portable devices we utilized. Only two typical PHEs were selected as study sites, where the diversity of semi-outdoor spaces is lacking. Sites with more diversified space types could be included in future. We also didn't conduct nighttime measurements due to the labor-consuming mobile measurement method. According to a previous study, the thermal environment pattern under tree canopy and shading shelter are different during daytime and nighttime [32]. Future work may incorporate comparisons between diurnal and nocturnal periods. Secondly, we applied physiological and empirical indices to evaluate thermal comfort in the targeted spaces, instead of directly measuring subjective thermal perception and sensation. And how building and greenery characteristics mediate subjective thermal perception through their influence on environment parameters, e.g., temperature, humidity, wind, and radiation, is therefore not quantified in this current study [33]. Additionally, considering that psychological and behavioral factors may have an influence on thermal sensation [84, 85], future studies are expected to adopt related research methodologies.

5. Conclusion

In this study, microclimate and thermal comfort during summertime heat waves in three types of public spaces were evaluated. We analyzed their relationship with 2D/3D building and greenery factors, and obtained an SVF threshold, which shows potential to be applied in practice under subtropical high-density urban setting. We conclude that.

- (1) Microclimate differences among three types of spaces are inconsistently significant across different times of day, while thermal comfort differences are constantly significant. Semi-outdoor spaces have the most favorable thermal condition, while the least in open squares. The mean overall enhancement of thermal comfort in vegetated and semi-outdoor spaces compared to open squares are 4.95 °C and 10.28 °C in PET, 2.95 °C and 6.65 °C in UTCI, and 1.48 °C and 2.84 °C in HKHI.
- (2) In outdoor spaces, i.e., vegetated spaces and open squares, 3D canopy and height factors play dominant role in determining microclimate and thermal comfort condition, with sky view factor (SVF) contributing the most. The key SVF threshold for effective thermal comfort enhancement is about 0.4, above which the climate-sensitive strategies are most needed. Effects of SVF contributed by buildings are only significant in open squares.
- (3) In semi-outdoor spaces, 2D composition factors perform greater impacts than 3D ones. Allocating proper building and greenery elements around semi-outdoor spaces is significant to provide a thermally comfortable environment in semi-outdoor spaces.

This study provides new empirical evidence under the context of summertime heat waves in subtropical residential areas, which can be referred to by urban and landscape designers when allocating building and greenery elements to adapt to future heat waves.

CRedit authorship contribution statement

Yilun Li: Writing – original draft, Methodology, Investigation, Formal analysis. **Wanlu Ouyang:** Writing – review & editing, Methodology. **Shi Yin:** Writing – review & editing, Software. **Zheng Tan:** Writing – review & editing. **Chao Ren:** Writing – review & editing, Supervision, Resources, Project administration, Funding acquisition, Conceptualization.

Declaration of competing interest

The authors declare that they have no known competing financial interests or personal relationships that could have appeared to influence the work reported in this paper.

Data availability

Data will be made available on request.

Acknowledgments

The study is supported by 2021/22 Theme-based Research Scheme (Ref-No: T22-504/21-R, named “Healthy and Resilient City with Pervasive LoCHs”) of Hong Kong Research Grants Council. We acknowledge Ms. Shu Yi, Ms. Guancong Ren, and Ms. Maoping Wang's assistance on data sampling. We also thank the editor and anonymous reviewers for their valuable suggestions.

Appendix A. Supplementary data

Supplementary data to this article can be found online at <https://doi.org/10.1016/j.buildenv.2023.110225>.

References

- [1] United In Science WMO, A Multi-Organization High-Level Compilation of the Most Recent Science Related to Climate Change, Impacts and Responses, 2022, 2022.
- [2] J. Zuo, S. Pullen, J. Palmer, H. Bennetts, N. Chileshe, T. Ma, Impacts of heat waves and corresponding measures: a review, *J. Clean. Prod.* 92 (2015) 1–12, <https://doi.org/10.1016/j.jclepro.2014.12.078>.
- [3] Heatwaves and Health WMO, Guidance on Warning-System Development, 2015.
- [4] P.J. Robinson, On the definition of a heat wave, *J. Appl. Meteorol.* 40 (4) (2001) 762–775, [https://doi.org/10.1175/1520-0450\(2001\)040<0762:Otdoah>2.0.Co;2](https://doi.org/10.1175/1520-0450(2001)040<0762:Otdoah>2.0.Co;2).
- [5] M.J. Hintz, C. Luederitz, D.J. Lang, H. von Wehrden, Facing the heat: a systematic literature review exploring the transferability of solutions to cope with urban heat waves, *Urban Clim.* 24 (2018) 714–727, <https://doi.org/10.1016/j.uclim.2017.08.011>.
- [6] V. Mehta, Evaluating public space, *J. Urban Des.* 19 (1) (2013) 53–88, <https://doi.org/10.1080/13574809.2013.854698>.
- [7] M. Hendel, K. Azos-Diaz, B. Tremeac, Behavioral adaptation to heat-related health risks in cities, *Energy Build.* 152 (2017) 823–829, <https://doi.org/10.1016/j.enbuild.2016.11.063>.
- [8] O. Potchter, P. Cohen, T.P. Lin, A. Matzarakis, A systematic review advocating a framework and benchmarks for assessing outdoor human thermal perception, *Sci. Total Environ.* 833 (2022), 155128, <https://doi.org/10.1016/j.scitotenv.2022.155128>.
- [9] D. Lai, W. Liu, T. Gan, K. Liu, Q. Chen, A review of mitigating strategies to improve the thermal environment and thermal comfort in urban outdoor spaces, *Sci. Total Environ.* 661 (2019) 337–353, <https://doi.org/10.1016/j.scitotenv.2019.01.062>.
- [10] S. Banerjee, G. Ching N. Y., S.K. Yik, Y. Dzyuban, P.J. Crank, R. Pek Xin Yi, W.T. L. Chow, Analysing impacts of urban morphological variables and density on outdoor microclimate for tropical cities: a review and a framework proposal for future research directions, *Build. Environ.* 225 (2022), <https://doi.org/10.1016/j.buildenv.2022.109646>.
- [11] M.M. Elzeni, A.A. Elmokadem, N.M. Badawy, Impact of urban morphology on pedestrians: a review of urban approaches, *Cities* 129 (2022), <https://doi.org/10.1016/j.cities.2022.103840>.
- [12] B. Yuan, L. Zhou, X. Dang, D. Sun, F. Hu, H. Mu, Separate and combined effects of 3D building features and urban green space on land surface temperature, *J. Environ. Manag.* 295 (2021), 113116, <https://doi.org/10.1016/j.jenvman.2021.113116>.
- [13] J. Yang, Y. Yang, D. Sun, C. Jin, X. Xiao, Influence of urban morphological characteristics on thermal environment, *Sustain. Cities Soc.* 72 (2021), <https://doi.org/10.1016/j.scs.2021.103045>.
- [14] D. Han, H. An, F. Wang, X. Xu, Z. Qiao, M. Wang, X. Sui, S. Liang, X. Hou, H. Cai, Y. Liu, Understanding seasonal contributions of urban morphology to thermal environment based on boosted regression tree approach, *Build. Environ.* 226 (2022), <https://doi.org/10.1016/j.buildenv.2022.109770>.
- [15] J. Chen, W. Zhan, S. Jin, W. Han, P. Du, J. Xia, J. Lai, J. Li, Z. Liu, L. Li, F. Huang, H. Ding, Separate and combined impacts of building and tree on urban thermal environment from two- and three-dimensional perspectives, *Build. Environ.* 194 (2021), <https://doi.org/10.1016/j.buildenv.2021.107650>.
- [16] J. Unger, Intra-urban relationship between surface geometry and urban heat island: review and new approach, *Clim. Res.* 27 (2004) 253–264, <https://doi.org/10.3354/cr027253>.

- [17] J. Zhang, Z. Li, Y. Wei, D. Hu, The impact of the building morphology on microclimate and thermal comfort—a case study in Beijing, *Build. Environ.* 223 (2022), <https://doi.org/10.1016/j.buildenv.2022.109469>.
- [18] J. Zhang, Z. Li, D. Hu, Effects of urban morphology on thermal comfort at the micro-scale, *Sustain. Cities Soc.* 86 (2022), <https://doi.org/10.1016/j.scs.2022.104150>.
- [19] Z. Wu, P. Dou, L. Chen, Comparative and combinative cooling effects of different spatial arrangements of buildings and trees on microclimate, *Sustain. Cities Soc.* 51 (2019), <https://doi.org/10.1016/j.scs.2019.101711>.
- [20] Z. Wu, L. Chen, Optimizing the spatial arrangement of trees in residential neighborhoods for better cooling effects: integrating modeling with in-situ measurements, *Landsc. Urban Plann.* 167 (2017) 463–472, <https://doi.org/10.1016/j.landurbplan.2017.07.015>.
- [21] Y. Yang, D. Zhou, Y. Wang, X. Meng, Z. Gu, D. Xu, X. Han, Planning method of centralized greening in high-rise residential blocks based on improvement of thermal comfort in summer, *Sustain. Cities Soc.* 80 (2022), <https://doi.org/10.1016/j.scs.2022.103802>.
- [22] Y. Li, D. Lin, Y. Zhang, Z. Song, X. Sha, S. Zhou, C. Chen, Z. Yu, Quantifying tree canopy coverage threshold of typical residential quarters considering human thermal comfort and heat dynamics under extreme heat, *Build. Environ.* 233 (2023), <https://doi.org/10.1016/j.buildenv.2023.110100>.
- [23] Y. Tian, W. Zhou, Y. Qian, Z. Zheng, J. Yan, The effect of urban 2D and 3D morphology on air temperature in residential neighborhoods, *Landsc. Ecol.* 34 (5) (2019) 1161–1178, <https://doi.org/10.1007/s10980-019-00834-7>.
- [24] J. Gamero-Salinas, N. Kishnani, A. Sánchez-Ostiz, A. Monge-Barrio, E. Benitez, Porosity, openness, and exposure: identification of underlying factors associated with semi-outdoor spaces' thermal performance and clustering in tropical high-density Singapore, *Energy Build.* 272 (2022), <https://doi.org/10.1016/j.enbuild.2022.112339>.
- [25] J. Gamero-Salinas, N. Kishnani, A. Monge-Barrio, J. López-Fidalgo, A. Sánchez-Ostiz, Evaluation of thermal comfort and building form attributes in different semi-outdoor environments in a high-density tropical setting, *Build. Environ.* 205 (2021), <https://doi.org/10.1016/j.buildenv.2021.108255>.
- [26] J. Gamero-Salinas, N. Kishnani, A. Monge-Barrio, J. López-Fidalgo, A. Sánchez-Ostiz, The influence of building form variables on the environmental performance of semi-outdoor spaces. A study in mid-rise and high-rise buildings of Singapore, *Energy Build.* 230 (2021), <https://doi.org/10.1016/j.enbuild.2020.110544>.
- [27] T. Huang, J. Niu, Y. Xie, J. Li, C.M. Mak, Assessment of “lift-up” design's impact on thermal perceptions in the transition process from indoor to outdoor, *Sustain. Cities Soc.* 56 (2020), <https://doi.org/10.1016/j.scs.2020.102081>.
- [28] J. Niu, J. Liu, T.-c. Lee, Z. Lin, C. Mak, K.-T. Tse, B.-s. Tang, K.C.S. Kwok, A new method to assess spatial variations of outdoor thermal comfort: onsite monitoring results and implications for precinct planning, *Build. Environ.* 91 (2015) 263–270, <https://doi.org/10.1016/j.buildenv.2015.02.017>.
- [29] T. Xi, Q. Li, A. Mochida, Q. Meng, Study on the outdoor thermal environment and thermal comfort around campus clusters in subtropical urban areas, *Build. Environ.* 52 (2012) 162–170, <https://doi.org/10.1016/j.buildenv.2011.11.006>.
- [30] K. Lyu, R. de Dear, A. Brambilla, A. Globa, Restorative benefits of semi-outdoor environments at the workplace: does the thermal realm matter? *Build. Environ.* 222 (2022) <https://doi.org/10.1016/j.buildenv.2022.109355>.
- [31] B. Cao, M. Luo, M. Li, Y. Zhu, Thermal comfort in semi-outdoor spaces within an office building in Shenzhen: a case study in a hot climate region of China, *Indoor Built Environ.* 27 (10) (2017) 1431–1444, <https://doi.org/10.1177/1420326x17728152>.
- [32] P.K. Cheung, C.Y. Jim, Comparing the cooling effects of a tree and a concrete shelter using PET and UTCI, *Build. Environ.* 130 (2018) 49–61, <https://doi.org/10.1016/j.buildenv.2017.12.013>.
- [33] R.-L. Hwang, T.-P. Lin, Thermal comfort requirements for occupants of semi-outdoor and outdoor environments in hot-humid regions, *Architect. Sci. Rev.* 50 (4) (2007) 357–364, <https://doi.org/10.3763/asre.2007.5043>.
- [34] J. Li, J. Niu, C.M. Mak, Study of Pedestrians' Mixed Thermal Responses when Experiencing Rapid and Simultaneous Variations in Sun and Wind Conditions in Urban Continuums, *Sustainable Cities and Society*, 2022, <https://doi.org/10.1016/j.scs.2022.104169>.
- [35] K. Mihara, S. Chen, T. Hasama, C.L. Tan, J.K. Wei Lee, N.H. Wong, Transient Thermal and Physiological Responses from Air-Conditioned Room to Semi-outdoor Space in the Tropics, *Building and Environment*, 2022, <https://doi.org/10.1016/j.buildenv.2022.109611>.
- [36] N. Kabisch, R. Kraemer, O. Masztalerz, J. Hemmerling, C. Püffel, D. Haase, Impact of summer heat on urban park visitation, perceived health and ecosystem service appreciation, *Urban For. Urban Green.* 60 (2021), <https://doi.org/10.1016/j.ufug.2021.127058>.
- [37] C. Du, W. Jia, M. Chen, L. Yan, K. Wang, How can urban parks be planned to maximize cooling effect in hot extremes? Linking maximum and accumulative perspectives, *J. Environ. Manag.* 317 (2022), 115346, <https://doi.org/10.1016/j.jenvman.2022.115346>.
- [38] M. Chen, W. Jia, L. Yan, C. Du, K. Wang, Quantification and mapping cooling effect and its accessibility of urban parks in an extreme heat event in a megacity, *J. Clean. Prod.* 334 (2022), <https://doi.org/10.1016/j.jclepro.2021.130252>.
- [39] H. Lee, H. Mayer, L. Chen, Contribution of trees and grasslands to the mitigation of human heat stress in a residential district of Freiburg, Southwest Germany, *Landsc. Urban Plann.* 148 (2016) 37–50, <https://doi.org/10.1016/j.landurbplan.2015.12.004>.
- [40] G. Maggiotto, A. Miani, E. Rizzo, M.D. Castellone, P. Piscitelli, Heat waves and adaptation strategies in a mediterranean urban context, *Environ. Res.* 197 (2021), 111066, <https://doi.org/10.1016/j.envres.2021.111066>.
- [41] H. Huang, P. Jie, Research on the characteristics of high-temperature heat waves and outdoor thermal comfort: a typical space in chongqing yuzhong district as an example, *Buildings-Basel* 12 (5) (2022), <https://doi.org/10.3390/buildings12050625>.
- [42] S. Yin, J. Hua, C. Ren, S. Liu, H. Lin, S. Huang, K. Wang, J. Ma, Y. Xiao, Impact of synoptic condition on urban microclimate variation: a measurement study in a humid subtropical city during summer season, *Urban Clim.* 47 (2023), <https://doi.org/10.1016/j.uclim.2022.101350>.
- [43] L.W. Siu, M.A. Hart, Quantifying urban heat island intensity in Hong Kong SAR, China, *Environ. Monit. Assess.* 185 (5) (2013) 4383–4398, <https://doi.org/10.1007/s10661-012-2876-6>.
- [44] J. Hua, X. Zhang, C. Ren, Y. Shi, T.-C. Lee, Spatiotemporal assessment of extreme heat risk for high-density cities: a case study of Hong Kong from 2006 to 2016, *Sustain. Cities Soc.* 64 (2021), <https://doi.org/10.1016/j.scs.2020.102507>.
- [45] Census and Statistics Department, in: 2021 Edition HKSAR Government. *Hong Kong Annual Digest of Statistics*, 2021. Hong Kong.
- [46] Housing Bureau, *Housing in Figures 2021*. <https://www.hb.gov.hk/eng/publications/housing/HIF2021.pdf> (accessed 1 March 2023).
- [47] Hong Kong Observatory. <https://www.hko.gov.hk/en/Observatorys-Blog/101805/Knowing-more-about-Very-Hot-Weather-Warning>. 2023 (accessed 1 March 2023).
- [48] K.L. Lee, Y.H. Chan, T.C. Lee, W.B. Goggins, E.Y. Chan, The development of the Hong Kong Heat Index for enhancing the heat stress information service of the Hong Kong Observatory, *Int. J. Biometeorol.* 60 (7) (2016) 1029–1039, <https://doi.org/10.1007/s00484-015-1094-7>.
- [49] ISO, BS EN ISO 7726:1998 *Ergonomics of the Thermal Environment — Instruments for Measuring Physical Quantities*, 1998.
- [50] W. Ouyang, Z. Liu, K. Lau, Y. Shi, E. Ng, Comparing different recalibrated methods for estimating mean radiant temperature in outdoor environment, *Build. Environ.* 216 (2022), <https://doi.org/10.1016/j.buildenv.2022.109004>.
- [51] Z. Liu, K.Y. Cheng, Y. He, C.Y. Jim, R.D. Brown, Y. Shi, K. Lau, E. Ng, Microclimatic measurements in tropical cities: systematic review and proposed guidelines, *Build. Environ.* 222 (2022), <https://doi.org/10.1016/j.buildenv.2022.109411>.
- [52] A. Lai, M. Maing, E. Ng, Observational studies of mean radiant temperature across different outdoor spaces under shaded conditions in densely built environment, *Build. Environ.* 114 (2017) 397–409, <https://doi.org/10.1016/j.buildenv.2016.12.034>.
- [53] K. Li, Y. Zhang, L. Zhao, Outdoor thermal comfort and activities in the urban residential community in a humid subtropical area of China, *Energy Build.* 133 (2016) 498–511, <https://doi.org/10.1016/j.enbuild.2016.10.013>.
- [54] W. Ouyang, T.E. Morakinyo, C. Ren, S. Liu, E. Ng, Thermal-irradiant performance of green infrastructure typologies: field measurement study in a subtropical climate city, *Sci. Total Environ.* 764 (2021), 144635, <https://doi.org/10.1016/j.scitotenv.2020.144635>.
- [55] O. Potchter, P. Cohen, T.P. Lin, A. Matzarakis, Outdoor human thermal perception in various climates: a comprehensive review of approaches, methods and quantification, *Sci. Total Environ.* 631–632 (2018) 390–406, <https://doi.org/10.1016/j.scitotenv.2018.02.276>.
- [56] W. Ouyang, T.E. Morakinyo, C. Ren, E. Ng, The cooling efficiency of variable greenery coverage ratios in different urban densities: a study in a subtropical climate, *Build. Environ.* 174 (2020), <https://doi.org/10.1016/j.buildenv.2020.106772>.
- [57] A. Matzarakis, F. Rutz, H. Mayer, Modelling radiation fluxes in simple and complex environments—application of the RayMan model, *Int. J. Biometeorol.* 51 (4) (2007) 323–334, <https://doi.org/10.1007/s00484-006-0061-8>.
- [58] A. Matzarakis, F. Rutz, H. Mayer, Modelling radiation fluxes in simple and complex environments: basics of the RayMan model, *Int. J. Biometeorol.* 54 (2) (2010) 131–139, <https://doi.org/10.1007/s00484-009-0261-0>.
- [59] R. Giridharan, S.S.Y. Lau, S. Ganesan, B. Givoni, Lowering the outdoor temperature in high-rise high-density residential developments of coastal Hong Kong: the vegetation influence, *Build. Environ.* 43 (10) (2008) 1583–1595, <https://doi.org/10.1016/j.buildenv.2007.10.003>.
- [60] C. Miao, S. Yu, Y. Hu, H. Zhang, X. He, W. Chen, Review of methods used to estimate the sky view factor in urban street canyons, *Build. Environ.* 168 (2020), <https://doi.org/10.1016/j.buildenv.2019.106497>.
- [61] P.P. Olea, P. Mateo-Tomas, A. de Frutos, Estimating and modelling bias of the hierarchical partitioning public-domain software: implications in environmental management and conservation, *PLoS One* 5 (7) (2010), e11698, <https://doi.org/10.1371/journal.pone.0011698>.
- [62] V.M. Muggeo, Estimating regression models with unknown break-points, *Stat. Med.* 22 (19) (2003) 3055–3071, <https://doi.org/10.1002/sim.1545>.
- [63] Y. Liu, J. Peng, Y. Wang, Efficiency of landscape metrics characterizing urban land surface temperature, *Landsc. Urban Plann.* 180 (2018) 36–53, <https://doi.org/10.1016/j.landurbplan.2018.08.006>.
- [64] P.K. Cheung, C.Y. Jim, Subjective outdoor thermal comfort and urban green space usage in humid-subtropical Hong Kong, *Energy Build.* 173 (2018) 150–162, <https://doi.org/10.1016/j.enbuild.2018.05.029>.
- [65] T.P. Lin, A. Matzarakis, Tourism climate and thermal comfort in sun moon lake, taiwan, *Int. J. Biometeorol.* 52 (4) (2008) 281–290, <https://doi.org/10.1007/s00484-007-0122-7>.
- [66] P. Brode, D. Fiala, K. Blazejczyk, I. Holmer, G. Jendritzky, B. Kampmann, B. Tinz, G. Havenith, Deriving the operational procedure for the universal thermal climate index (UTCI), *Int. J. Biometeorol.* 56 (3) (2012) 481–494, <https://doi.org/10.1007/s00484-011-0454-1>.

- [67] H. Taha, Urban climates and heat islands: albedo, evapotranspiration, and anthropogenic heat, *Energy Build.* 25 (2) (1997) 99–103, [https://doi.org/10.1016/s0378-7788\(96\)00999-1](https://doi.org/10.1016/s0378-7788(96)00999-1).
- [68] X. Zhang, L. Zhao, L. Yao, X. Zhong, P. Ren, Investigating the micro-scale thermal effects of natural underlying surfaces on adjacent spaces in a subtropical zone with an optimized method, *Build. Environ.* 222 (2022), <https://doi.org/10.1016/j.buildenv.2022.109382>.
- [69] Y. Du, C.M. Mak, T. Huang, J. Niu, Towards an integrated method to assess effects of lift-up design on outdoor thermal comfort in Hong Kong, *Build. Environ.* 125 (2017) 261–272, <https://doi.org/10.1016/j.buildenv.2017.09.001>.
- [70] X. Zhang, K.T. Tse, A.U. Weerasuriya, S.W. Li, K.C.S. Kwok, C.M. Mak, J. Niu, Z. Lin, Evaluation of pedestrian wind comfort near 'lift-up' buildings with different aspect ratios and central core modifications, *Build. Environ.* 124 (2017) 245–257, <https://doi.org/10.1016/j.buildenv.2017.08.012>.
- [71] L.A. Ruefenacht, J.A. Acera, Strategies for Cooling Singapore A Catalogue of 80+ Measures to Mitigate Urban Heat Island and Improve Outdoor Thermal Comfort, 2017, <https://doi.org/10.3929/ethz-b-000258216>.
- [72] Y. Wang, F. Bakker, R. de Groot, H. Wortche, R. Leemans, Effects of urban trees on local outdoor microclimate: synthesizing field measurements by numerical modelling, *Urban Ecosyst.* 18 (4) (2015) 1305–1331, <https://doi.org/10.1007/s11252-015-0447-7>.
- [73] W. Chen, J. Zhang, X. Shi, S. Liu, Impacts of building features on the cooling effect of vegetation in community-based MicroClimate: recognition, measurement and simulation from a case study of Beijing, *Int. J. Environ. Res. Publ. Health* 17 (23) (2020), <https://doi.org/10.3390/ijerph17238915>.
- [74] M. Taleghani, Outdoor thermal comfort by different heat mitigation strategies- A review, *Renew. Sustain. Energy Rev.* 81 (2018) 2011–2018, <https://doi.org/10.1016/j.rser.2017.06.010>.
- [75] M. Jiao, W. Zhou, Z. Zheng, J. Yan, J. Wang, Optimizing the shade potential of trees by accounting for landscape context, *Sustain. Cities Soc.* 70 (2021), <https://doi.org/10.1016/j.scs.2021.102905>.
- [76] J. Park, J.-H. Kim, W. Sohn, D.-K. Lee, Urban cooling factors: do small greenspaces outperform building shade in mitigating urban heat island intensity? *Urban For. Urban Green.* 64 (2021) <https://doi.org/10.1016/j.ufug.2021.127256>.
- [77] H. Yan, F. Wu, X. Nan, Q. Han, F. Shao, Z. Bao, Influence of view factors on intra-urban air temperature and thermal comfort variability in a temperate city, *Sci. Total Environ.* 841 (2022), 156720, <https://doi.org/10.1016/j.scitotenv.2022.156720>.
- [78] J. Hua, M. Cai, Y. Shi, C. Ren, J. Xie, L.C.H. Chung, Y. Lu, L. Chen, Z. Yu, C. Webster, Investigating pedestrian-level greenery in urban forms in a high-density city for urban planning, *Sustain. Cities Soc.* 80 (2022), <https://doi.org/10.1016/j.scs.2022.103755>.
- [79] S. Chen, N.H. Wong, W. Zhang, M. Ignatius, The impact of urban morphology on the spatiotemporal dimension of estate-level air temperature: a case study in the tropics, *Build. Environ.* 228 (2023), <https://doi.org/10.1016/j.buildenv.2022.109843>.
- [80] B. Abdi, A. Hami, D. Zarehaghi, Impact of small-scale tree planting patterns on outdoor cooling and thermal comfort, *Sustain. Cities Soc.* 56 (2020), <https://doi.org/10.1016/j.scs.2020.102085>.
- [81] U. Berardi, Z. Jandaghian, J. Graham, Effects of greenery enhancements for the resilience to heat waves: a comparison of analysis performed through mesoscale (WRF) and microscale (Envi-met) modeling, *Sci. Total Environ.* 747 (2020), 141300, <https://doi.org/10.1016/j.scitotenv.2020.141300>.
- [82] N.B. Morris, G.K. Chaseling, T. English, F. Gruss, M.F.B. Maideen, A. Capon, O. Jay, Electric fan use for cooling during hot weather: a biophysical modelling study, *Lancet Planet. Health* 5 (6) (2021) e368–e377, [https://doi.org/10.1016/S2542-5196\(21\)00136-4](https://doi.org/10.1016/S2542-5196(21)00136-4).
- [83] F. Tartarini, S. Schiavon, O. Jay, E. Arens, C. Huizenga, Application of Gagge's energy balance model to determine humidity-dependent temperature thresholds for healthy adults using electric fans during heatwaves, *Build. Environ.* 207 (2022), <https://doi.org/10.1016/j.buildenv.2021.108437>.
- [84] J. Liu, J. Jiao, Y. Xie, Y. Xu, B. Lin, Assessment on the expectation for outdoor usage and its influencing factors, *Urban Clim.* 42 (2022), <https://doi.org/10.1016/j.uclim.2022.101132>.
- [85] Y. Geng, B. Hong, M. Du, T. Yuan, Y. Wang, Combined effects of visual-acoustic-thermal comfort in campus open spaces: a pilot study in China's cold region, *Build. Environ.* 209 (2022), <https://doi.org/10.1016/j.buildenv.2021.108658>.